

SPEED OF MERIDIONAL FLOWS AND MAGNETIC FLUX TRANSPORT ON THE SUN

MICHAL ŠVANDA,^{1,2} ALEXANDER G. KOSOVICHEV,³ AND JUNWEI ZHAO³

Received 2007 September 2; accepted 2007 October 2; published 2007 October 19

ABSTRACT

We use the magnetic butterfly diagram to determine the speed of the magnetic flux transport on the solar surface toward the poles. The manifestation of the flux transport is clearly visible as elongated structures extended from the sunspot belt to the polar regions. The slopes of these structures are measured and interpreted as meridional magnetic flux transport speed. Comparison with the time-distance helioseismology measurements of the mean speed of the meridional flows at a depth of 3.5–12 Mm shows a generally good agreement, but the speeds of the flux transport and the meridional flow are significantly different in areas occupied by the magnetic field. The local circulation flows around active regions, especially the strong equatorward flows on the equatorial side of active regions, affect the mean velocity profile derived by helioseismology but do not influence the magnetic flux transport. The results show that the mean longitudinally averaged meridional flow measurements by helioseismology may not be used directly in solar dynamo models for describing the magnetic flux transport, and that it is necessary to take into account the longitudinal structure of these flows.

Subject headings: Sun: activity — Sun: atmospheric motions — Sun: magnetic fields

1. INTRODUCTION

The largest scale velocity fields on the Sun consist of differential rotation and meridional circulation. The differential rotation is defined as an integral of the zonal (east-west) component of the velocity field depending on the solar latitude, b , and radius. The meridional flow is calculated as an integral of the north-south component of the velocity field, generally depending again on the latitude and radius. Both the differential rotation and meridional circulation are the key ingredients of the solar dynamo. The differential rotation plays an important role in generating and strengthening of toroidal magnetic field inside the Sun, while the meridional flow transports the magnetic flux toward the solar poles resulting in cyclic polar field reversals (for a recent review, see Brandenburg & Subramanian 2005).

The meridional flux transport seems to be an essential agent influencing the length, strength, and other properties of solar magnetic cycles. Generally, the slower the meridional flows are, the longer the next magnetic cycle that is expected. Dynamo models showed that the turnaround time of the meridional cell is between 17 and 21 yr, and that the global dynamo may have some kind of memory lasting longer than one cycle (Dikpati et al. 2006).

The speed of the meridional flow and its variation with the solar cycle measured by local helioseismology in the subsurface layers of the Sun were used as an input in the recent flux-transport models (Dikpati & Gilman 2006). In local helioseismology measurements (e.g., Zhao & Kosovichev 2004; González Hernández et al. 2006), the meridional flow was derived from a general subsurface flow field by averaging the north-south component of the plasma velocity over longitude for a Carrington rotation period. The studies revealed that the mean meridional flow varied with the solar activity cycle. These variations may significantly affect solar-cycle predictions based on the solar dynamo models, which assume that the magnetic

flux is transported with the mean meridional flow speed (Dikpati & Gilman 2006).

Our goal is to verify this assumption and to investigate the relationship between the subsurface meridional flows and the flux transport. In this study, we show that the mean meridional flows derived from the time-distance helioseismology subsurface flow maps are affected by strong local flows around active regions in the activity belts. These local flows have much less significant effect on the magnetic flux transport.

2. METHOD OF MEASUREMENTS

The magnetic field data were obtained from Kitt Peak synoptic maps of longitudinal magnetic field. The magnetic butterfly diagram is continuously constructed from synoptic magnetic maps measured at the National Solar Observatory by averaging the magnetic flux in longitude at each latitude for each solar rotation since 1976 (Hathaway 2003).

At midlatitudes of the magnetic butterfly diagram (Fig. 1*a*), between the active region zone and polar regions, we clearly see elongated structures corresponding to the poleward magnetic flux transport. The aim of our method is to measure the slopes of these structures and to derive the speed of the meridional magnetic flux transport.

In addition to the large-scale structures, the original diagram contains small-scale, relatively short-lived local magnetic field structures, which appear as a “noise” in the diagram. To improve the signal-to-noise ratio for the magnetic flux structures we applied a frequency band-pass filter for the frequencies between $1.06 \times 10^{-8} \text{ s}^{-1}$ (period of 1093 days) and $3.17 \times 10^{-7} \text{ s}^{-1}$ (period of 36.5 days). The filtering procedure is performed separately for each individual latitudinal cut on the diagram. We also tried other methods of enhancement of structures and found that they all provided comparable results. The difference between the original butterfly diagram and the filtered one can be seen in Figures 1*a* and 1*b*. The flux-transport elongated structures are more easily visible after the filtering and therefore more suitable for analysis.

The meridional flux transport speed is measured on the basis of cross-correlation of two rows, which are assumed to be similar in shape, but the positions of structures differ due to their meridional transport. We cross-correlate pairs of rows

¹ Astronomical Institute (v.v.i.), Academy of Sciences, Ondřejov Observatory, CZ-25165, Czech Republic; michal@astronomie.cz.

² Astronomical Institute, Charles University, Prague, CZ-18200, Czech Republic.

³ W. W. Hansen Experimental Physics Laboratory, Stanford University, Stanford, CA 94305-4085; sasha@sun.stanford.edu, junwei@sun.stanford.edu.

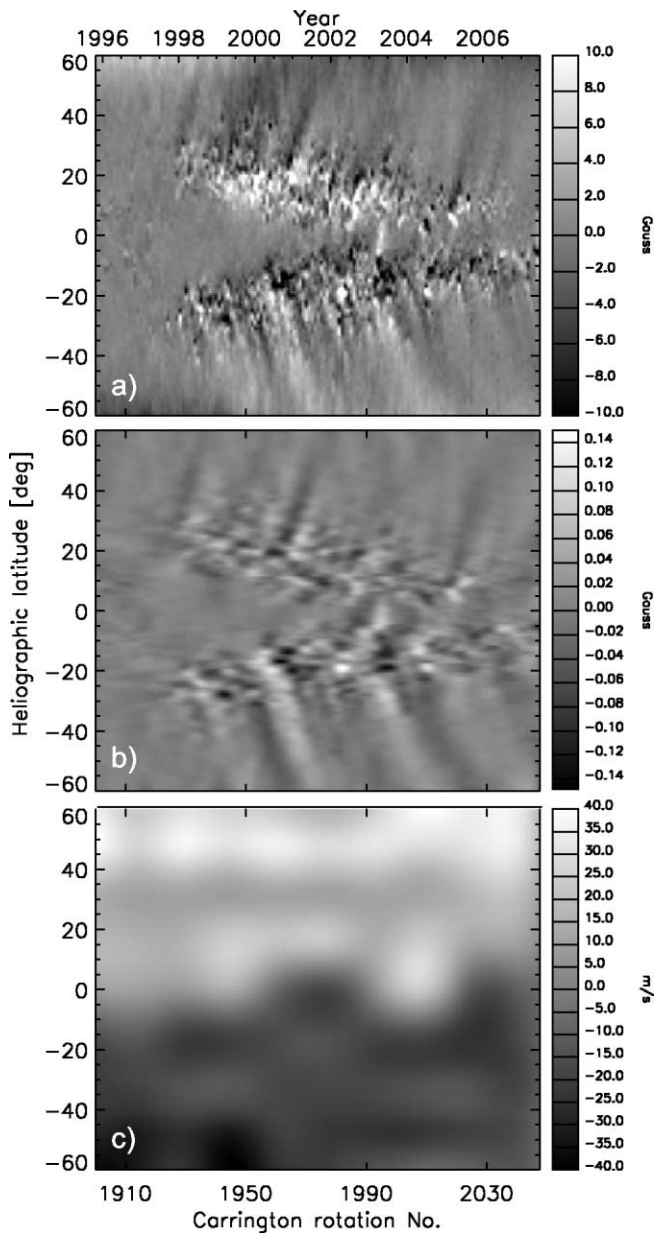


FIG. 1.—(a) Magnetic butterfly diagram for cycle 23. (b) Filtered magnetic butterfly diagram showing enhancements of the flux transport elongated structures. (c) Measured meridional flux transportation speed (in the south-north direction) for Carrington rotations 1900–2048.

separated by heliographic latitude Δb in a sliding window with the size of 55 Carrington rotations. The edges of the correlation window are apodized by a smooth function to avoid the boxcar effects. The extremal position is calculated as a maximum of the parabolic fit of the set of correlation coefficients of correlated windows in five discrete displacements. If the distribution of the correlation coefficients does not have a maximum, or if the R^2 is too low (under 0.8), the meridional velocity in this pixel is not evaluated. We have chosen $\Delta b = 5^\circ$ as the best tradeoff between the spatial resolution and precision.

To make the procedure more robust, we average the calculated meridional velocity for five consecutive frames separated by 0.5° and centered at Δb from the studied row. If any of the speeds in the averaged five rows is far out of the expected range (-60 to $+60$ m s^{-1}), then it is not used in the averaging. From the fit, the accuracy of the measured flow speed is evaluated, and the maximum value of the set of five independent

measurements at different rows is taken. The same procedure is done with the processed map rotated by 180° to avoid any possible preferences in the direction determination, and both results are averaged. The measured errors were taken as the maximum value of both independent measurements.

For the ongoing analysis, only the speeds that were measured with the error lower than 3 m s^{-1} were taken into account. This criterion and some failures of the slope measurement introduce gaps in the data, which we need to fill. For this purpose we need to determine the best continuous differentiable field that approximates the data. The determination of such a field can be done in various ways, but we wish to avoid possible artifacts. For filling the gaps we used the multiresolution analysis. It is based on wavelet analysis, and we have chosen the Daubechies wavelet due to its compact support. This property is important since it minimizes edge effects. Moreover, using these wavelets also preserves the location of zero-crossing and maxima of the signal during the analysis. Daubechies are claimed to be very stable in the noisy environments. For details see Rieutord et al. (2007).

The reconstructed meridional flux transport speed map can be seen in Figure 1c. The flux transport remains poleward during the whole studied period.

For the comparison between the meridional flow obtained from time-distance helioseismology (Zhao & Kosovichev 2004) and the magnetic flux transport from our method, we have calculated the averaged values of both quantities in bins of 10 heliographic degrees. For 1996–2006, only 11 Carrington rotations have been evaluated (one per year) by time-distance helioseismology using the full-disk dynamics data from the MDI instrument on board the *SOHO* spacecraft. These data are available only for approximately two months per year. We compared the measurements of the magnetic flux transport and the meridional flows in those particular nonconsecutive Carrington rotations. The plots are displayed in Figure 2.

3. RESULTS

The magnetic flux transport speed and the mean meridional flow speed obtained from helioseismology are very similar (correlation coefficients are in a range of 0.7–0.9). We have to keep in mind that while the time-distance meridional circulation profiles represent the behavior of the plasma during particular Carrington rotations, the magnetic butterfly diagram tracking profiles represent the flux transport smoothed over 10 Carrington rotations. Therefore, the agreement cannot be perfect in principle. To make our results more accurate, the continuous helioseismic data are needed.

The speeds of the meridional flux transport in the near-equatorial region are less reliable, since the elongated structures in the magnetic butterfly diagram extend from the activity belts toward poles. In the equatorial region, significant parts of the measurements were excluded from the analysis due to their large measured error. The gaps were filled using multiresolution analysis from well-measured points. Although the results seem reasonable here, their lower reliability has to be kept in mind. The original data are constructed from the images obtained with low resolution with the orthographical projection to disk. Therefore, values above the latitude of 50° are impacted by the projection effect, which reduces the spatial resolution and may cause an apparent increase of the measured meridional flux transport speed. This effect should be reduced if the higher resolution data would be used.

During the minimum of solar activity (such as CR 1911,

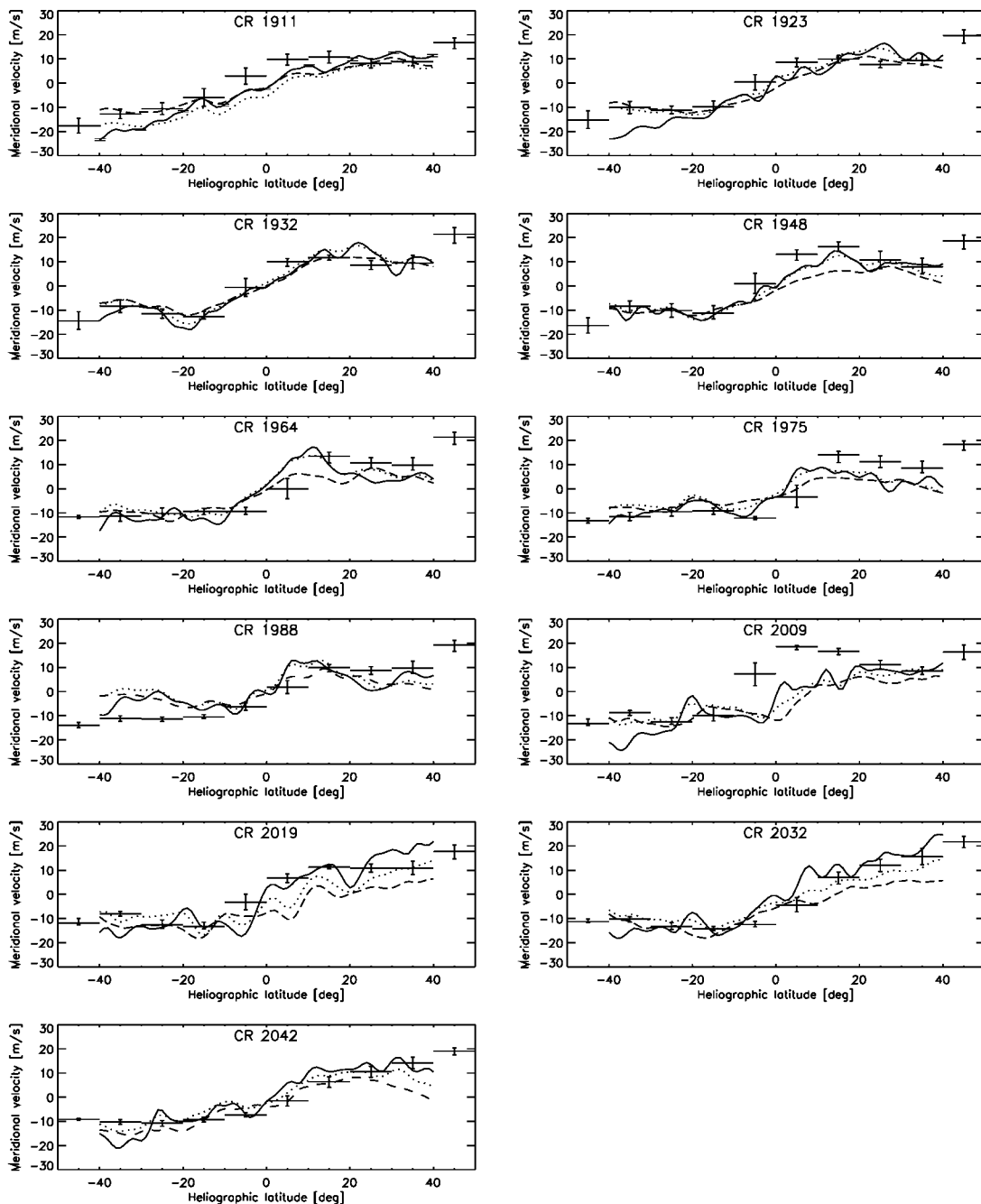


FIG. 2.—Longitudinally averaged meridional flow speed measured for a set of Carrington rotations by time-distance helioseismology and from the magnetic butterfly diagram. The solid line plots the time-distance mean meridional flow at 3–4.5 Mm depth, the dotted line at 6–9 Mm, and the dashed line at 9–12 Mm. The dots with error bars represent the 10° bin-averaged values of the flux transport speed derived from the magnetic butterfly diagram (Fig. 1a). Error bars of time-distance measurements are included for reference in CR 1911 (for details, see Zhao & Kosovichev 2004).

1923, or 2032), the profile of the meridional flux transport speed is very consistent with the mean longitudinally averaged profile of the meridional flow from helioseismology. The best agreement is found for depth of 9–12 Mm. This suggests that the flux transport may be influenced by flows in the deeper layers.

With increasing magnetic activity in the photosphere of the Sun, the gradient of the mean meridional circulation profile derived from time-distance helioseismology becomes steeper. This is consistent with the results obtained by numerical simulations by Brun (2004). The simulations show that with increasing magnetic activity, the Maxwell stresses oppose the Reynolds stresses, causing an acceleration of the meridional circulation and deceleration of the rotation in low latitudes. Our

measurements show that the variations of the slope of the mean meridional flux transport speed in latitude are lower with the progression of the solar cycle.

When the large active regions emerge in the activity belt, the flow toward the equator is formed on the equatorial side of the magnetic regions (see, e.g., the subsurface flow map in Fig. 3a). This equatorward flow acts as a countercell of the meridional flow (present at the same longitudes as the corresponding magnetic region) and causes a decrease of the mean meridional flow amplitude in the activity belt. This behavior is noted in all studied cases recorded during 11 nonconsecutive solar rotations, for which the dynamics data useful for helioseismic inversion exist. Therefore, the formation of the apparent

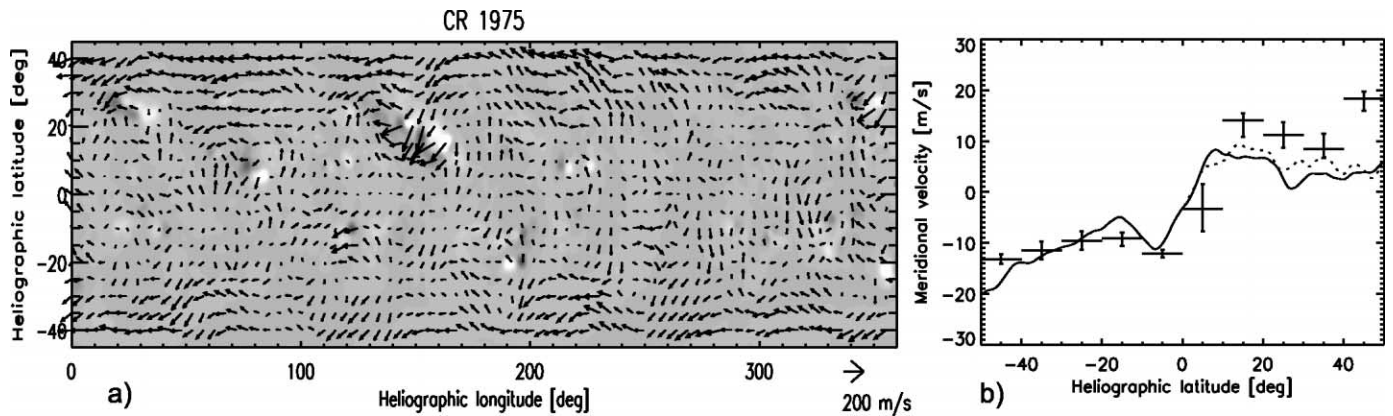


FIG. 3.—(a) Large-scale flow map at depth 3–4.5 Mm for Carrington rotation 1975 (2001 April) and the corresponding MDI magnetogram in the gray-scale background. Large-scale flows toward the equator in the magnetic regions are visible around the large active region. (b) The longitudinally averaged meridional circulation profile for the same Carrington rotation. The southern hemisphere depicts almost no magnetic activity, so the meridional circulation profile obtained by averaging the time-distance flow map (*solid line*) almost fits the magnetic flux transport profile (points with error bars) there, while on the northern hemisphere they differ. After masking the magnetic regions on the northern hemisphere, the recalculated profile (*dotted line*) tends to fit the butterfly tracking profile also on the northern hemisphere.

countercell seems to be a common property of all large active regions in depths 3–12 Mm.

Flows in this countercell do not influence the magnetic flux transport, which can be demonstrated when the magnetic region is excluded from the synoptic map (Fig. 3b). The calculated meridional circulation profile is then closer to the profile of the meridional flux transport speed derived from the magnetic butterfly diagram.

4. CONCLUSIONS

We have compared the measurements of the meridional speed derived from two different techniques: by time-distance local helioseismology and by measuring the flux transport speed using the magnetic butterfly diagram. We have found that the results agree quite well in general, but they differ in regions occupied by local magnetic fields. The detailed flow maps from helioseismology show that this is partly due to the presence of meridional countercells at the equatorial side of magnetic regions, which influence the time-distance–derived meridional flow profile, but does not influence the magnetic flux transport.

We have studied 11 nonconsecutive Carrington rotations covering one solar cycle. The effect of the local flows around active regions and especially on their equatorial side is noted

in all the studied cases. Therefore, this behavior seems to be a common property of the subsurface dynamics around active regions located in the activity belt. However, we have to keep in mind that both data sets are not directly comparable, since the time-distance flow maps represent the behavior of flows during one Carrington rotation, while the butterfly diagram tracking procedure provide results averaged over a few Carrington rotations. The more homogeneous data for local helioseismology are needed to study this effect in more detail.

The results show that the speed of the magnetic flux transport toward the solar poles may significantly deviate from the longitudinally averaged meridional flow speed derived from local helioseismology measurements, which are affected by local circulation flows around active regions in the activity belt. Therefore, using the longitudinally averaged meridional flow profile from helioseismology in the solar cycle models for description the flux transport is not justified. The longitudinal structure of these flows should be taken into account.

M. Š. would like to gratefully acknowledge ESA-PECS for the support under grant 8030, the Ministry of Education of the Czech Republic under Research Program MSM0021620860, and Stanford Solar Physics Group for support and hospitality.

REFERENCES

- Brandenburg, A., & Subramanian, K. 2005, *Phys. Rep.*, 417, 1
 Brun, A. S. 2004, *Sol. Phys.*, 220, 333
 Dikpati, M., & Gilman, P. A. 2006, *ApJ*, 649, 498
 Dikpati, M., de Toma, G., & Gilman, P. A. 2006, *Geophys. Res. Lett.*, 33, 5102
 González Hernández, I., Komm, R., Hill, F., Howe, R., Corbard, T., & Haber, D. A. 2006, *ApJ*, 638, 576
 Hathaway, D. H. 2003, in *Proc. SOHO 12/GONG+2002, Local and Global Helioseismology: The Present and Future*, ed. H. Sawaya-Lacoste (ESA SP-517; Noordwijk: ESA), 87
 Rieutord, M., Roudier, T., Roques, S., & Ducottet, C. 2007, *A&A*, 471, 687
 Zhao, J., & Kosovichev, A. G. 2004, *ApJ*, 603, 776